

# Multispectral optical tweezers for biochemical fingerprinting of CD9-positive exosome subpopulations

Randy P. Carney,<sup>\*,†</sup> Sidhartha Hazari,<sup>†</sup> Macalstair Colquhoun,<sup>†</sup> Di Tran,<sup>†</sup> Billanna Hwang,<sup>‡</sup> Michael S. Mulligan,<sup>‡</sup> James D. Bryers,<sup>¶</sup> Eugenia Girda,<sup>§</sup> Gary S. Leiserowitz,<sup>§</sup> Zachary J. Smith,<sup>||</sup> and Kit S. Lam<sup>\*,†,⊥</sup>

<sup>†</sup>*Department of Biochemistry and Molecular Medicine, University of California Davis, Sacramento, CA 95817, USA*

<sup>‡</sup>*Department of Surgery, University of Washington, 850 Republican Street, Seattle, WA, USA 98195-0005*

<sup>¶</sup>*Department of Bioengineering, University of Washington, 3720 15th Ave NE, Seattle, WA 98195, USA.*

<sup>§</sup>*Division of Gynecologic Oncology, University of California Davis Medical Center, Sacramento, California 98517, USA*

<sup>||</sup>*University of Science and Technology of China, Department of Precision Machinery and Precision Instrumentation, Hefei, Anhui, China 230027*

<sup>⊥</sup>*Division of Hematology/Oncology, University of California Davis Cancer Center, Sacramento, CA 95817, USA*

E-mail: rcarney@ucdavis.edu; kslam@ucdavis.edu

## Supporting Information

### Materials and Methods

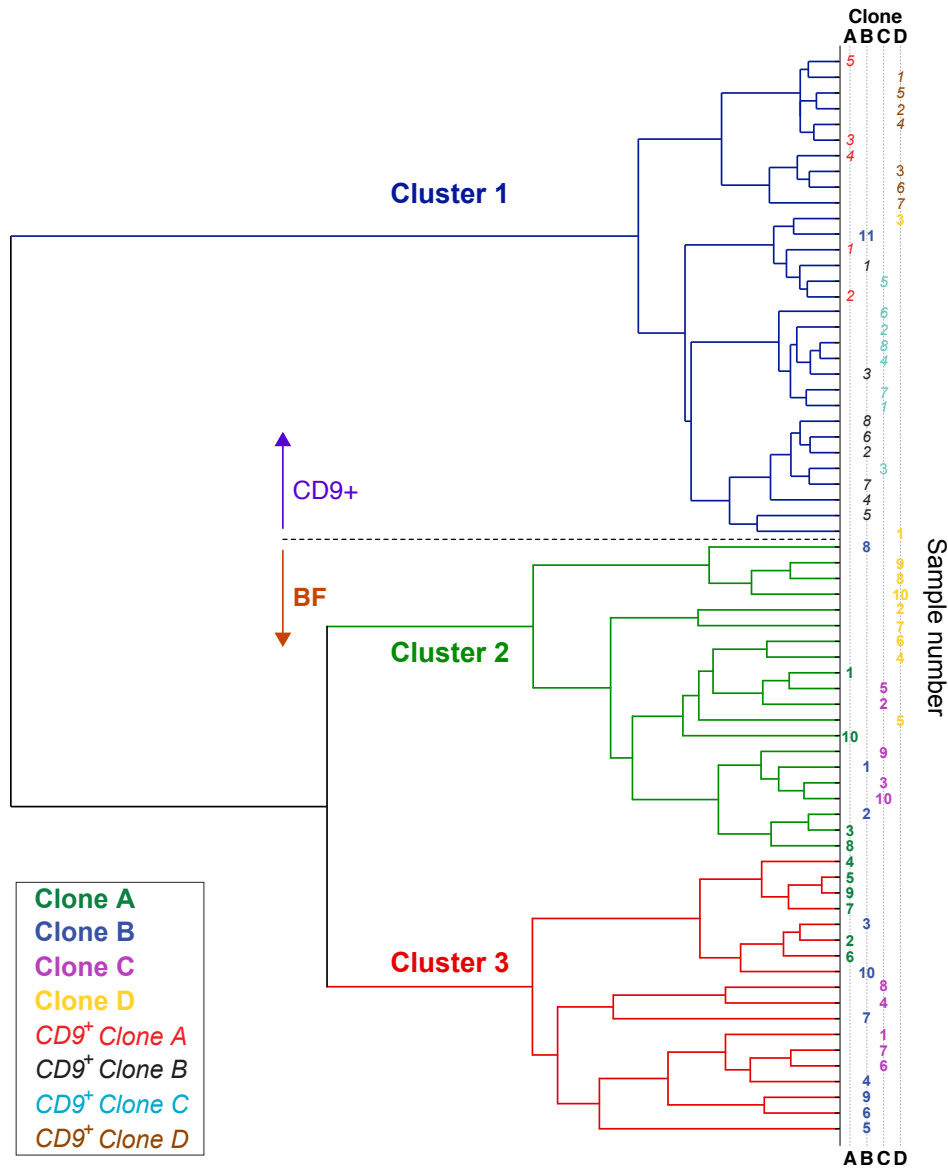
All chemicals were purchased from commercial suppliers and used without further purification. Cholesterol and the DOPC lipid used in this study (1,2-1,2-dioleoyl-sn-glycero-3-phosphocholine) were purchased from Avanti Polar Lipids, Inc. (Alabaster, AL). Anti-CD9-FITC was purchased from Abcam (Cambridge, MA). Unless otherwise noted, all other reagents and materials were purchased from Sigma-Aldrich Corp. (St. Louis, MO).

### Multispectral optical tweezers setup

785 nm laser light (CrystalLaser, Reno, NV) is coupled to a 60X, 1.2NA water immersion objective on an inverted microscope (Olympus IX-71). Brightfield images were illuminated by an

Olympus TH4-100 lamp. Fluorescence images were illuminated by mercury lamp. A spectrophotometer grating setting of 600 lp/mm was used, providing a resolution of approximately 5 wavenumbers.

Manual movement of the stage and focus height enabled vesicle trapping. To minimize background from the quartz, trapped vesicles were slowly brought up away the slide surface. To keep data consistent and accurate, we chose to avoid trapping particles with rough perimeters or whose tumbling motion could be clearly seen, both of which we believed indicators of an aggregate. An additional issue we encountered was the tendency of trapped particles to fall out of the trap before completion. To ensure particles remained in place for the duration of the Raman scattering detection, we routinely switch back to the camera following Raman scattering detection to check that the par-

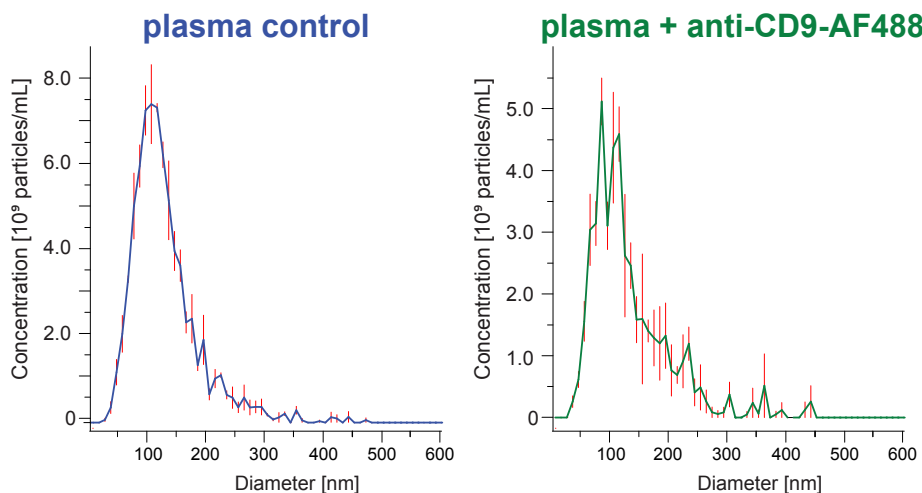


Supporting Figure. 1: Dendrogram showing the clustering result using the first 10 principal components across the entire dataset. Each terminus represents an individual vesicle. The spacing between dendrogram branches scales with dissimilarities in PC score. The major three clusters are color coded as in Figure 2d in the main text.

ticle is still trapped. Finally, to be sure we did not trap the same vesicle more than once, care was taken to move far away from the previous trapped vesicle following its release.

For a typical measurement, a 20  $\mu\text{L}$  drop containing a dilute sample of exosomes ( $10^5$  particles/mL as measured by NTA) was deposited on a quartz disc (SPI Supplies, 0.18 mm round x 0.15 mm thick) placed on a translational stage positioned over the objective lens. Once trapped, five 60-s integrations were taken to generate the final Raman spectra. DT-Acquire

software was used to observe the live feed from the video camera. Winspec software was used for recording spectra from the Raman detector. A processed dataset, i.e. cosmic ray removal, background-correction, and smoothing, all performed by a custom Matlab (Mathworks) script based on the built-in 'pca' function, which decomposes the dataset down into the scores and loadings. For hierarchical clustering, the input to linkage is the first 10 scores from the PCA decomposition. Scores with  $N > 10$  were typically corrupted by noise and removed. Fits of



Supporting Figure. 2: Post ultracentrifugation purification control. To examine the effect of an additional round of ultracentrifugation purification post antibody labeling, we examined the NTA size distributions for ovarian cancer plasma derived EVs previously purified by ultracentrifugation. The size distribution of the EVs subjected to another round of ultracentrifugation (a) did not significantly deviate from EVs pre-incubated with anti-CD9-AF488 antibody (b).

principle component cluster spectra to chemical standards were performed via least-squares modeling. More details concerning the analytical methodology can be found in a previous study.<sup>1</sup>

### Cell culture, exosome isolation and characterization

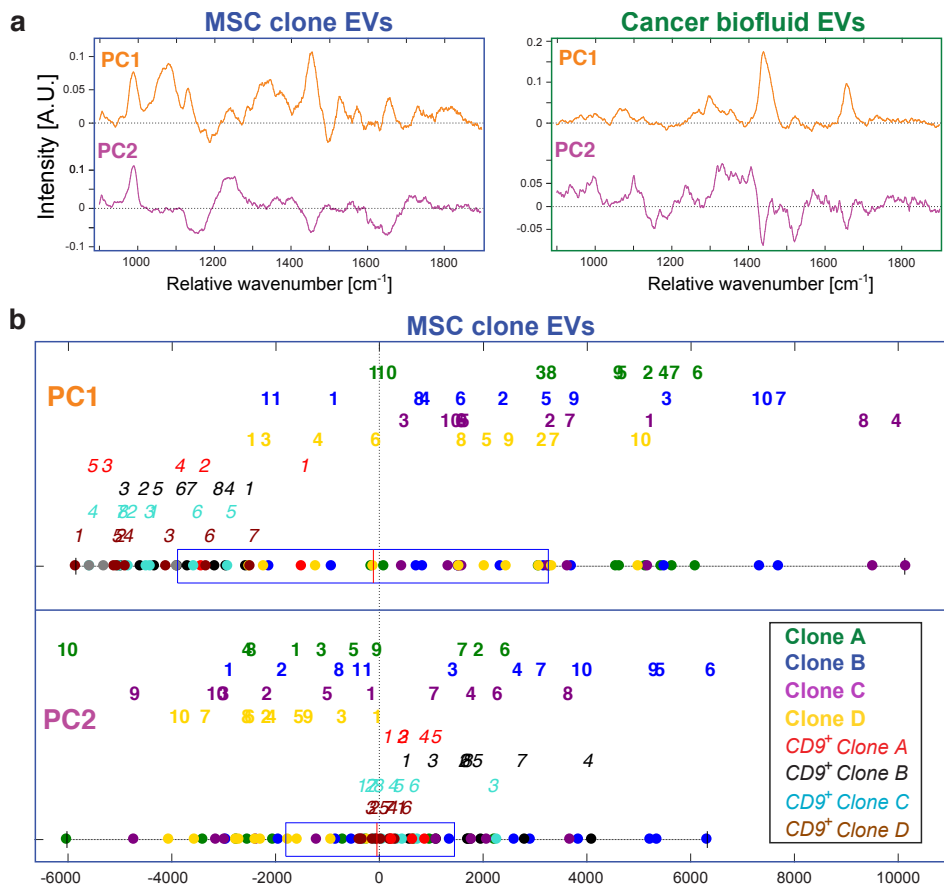
Four rat mesenchymal stromal cell (MSCs) lines were generated as previously described.<sup>2</sup> Briefly, bone marrow was isolated from adult rats, with buffy coats plated on plastic adherent tissue culture plates at a density of  $1.0 \times 10^6$  cells  $mL^{-1}$ . Primary adherent cells were exposed to LXS-16 E6E7 retrovirus for 2 hr and  $4 \mu g mL^{-1}$  polybrene. Virus containing medium was removed and adherent cells were incubated with medium containing polybrene for an additional 5 hr. All clones expressed CD73, CD90, CD105, and CD166, with no expression of CD14, CD34, and C45. MSC clones were assessed for differentiation potential using adipogenic and osteogenic differentiation kits (Trevigen, Gaithersburg, MD).

For exosome isolation, MSC cell line clones were cultured with RPMI medium containing 10% EV-depleted FBS (pre-cleared at  $100,000 \times g$ ,  $4^\circ C$ , 18 hr), to ensure that the resulting

EVs originate from the MSC cells. After 48 hr the cell culture medium is harvested and centrifuged at (i)  $2000 \times g$ , 10 min to remove cells and large debris, (ii)  $10,000 \times g$ , 30 min to remove microparticles and (iii)  $2 \times 100,000 \times g$ , 2 hr, to remove contaminating protein.<sup>3</sup> The resulting pellet was dissolved in a minimal amount of PBS ( $20 \mu L$  PBS per 5 million cells cultured) and frozen at  $-80^\circ C$  for up to month before analysis by MS-OTs.

Exosomes were isolated from blood and ascites on the same day of collection from the patient. Whole blood was collected in a lavender-capped plastic tube coated with the anticoagulant EDTA to prevent clotting, and carefully transported on ice to the lab for processing. 4 mL of whole blood was centrifuged at  $2,000 \times g$ ,  $4^\circ C$ , 15 min to separate plasma, which was carefully removed by Pasteur pipette to a cooled polypropylene tube. From here, plasma and ascites were subjected to the centrifugation steps (i - iii) outlined above for cell culture supernatant.

For antibody labeling, exosomes were mixed with a 1:100 dilution of anti-CD9-FITC antibody in MilliQ- $H_2O$ . After overnight incubation at  $4^\circ C$  under gentle rotation, the exosome solution was centrifuged at  $100,000 \times g$  for 2 hr



Supporting Figure. 3: (a) The first (orange) and second (purple) principal component loading vectors, calculated from the full EV spectral data set across either the four MSC clones (left) or the cancer biofluid sources (right). (b) One-dimensional first and second principal component scores for each single trapped MSC-vesicle, color coded according to clonal membership. Italics denote CD9<sup>+</sup> vesicles trapped under fluorescence examination.

to remove unbound antibody. The pellet was re-dissolved in 20  $\mu$ L PBS for immediate MS-OTs measurement. The ratio of protein concentration (by BCA assay) and number concentration/size distribution (by NTA) was used to ensure our preparations were relatively pure of excess free protein or other contaminating factors.<sup>4</sup> Procedures for BCA assay and NTA were performed as reported previously.<sup>1</sup>

## References

- (1) Smith, Z. J.; Lee, C.; Rojalin, T.; Carney, R. P.; Hazari, S.; Knudson, A.; Lam, K.; Saari, H.; Ibañez, E. L.; Vitala, T. et al. *J. Extracell. Vesicles* **2015**, *4*, DOI: 10.3402/jev.v4.28533.
- (2) Hwang, B.; Liles, W. C.; Waworuntu, R.; Mulligan, M. S. *J. Thorac. Cardiovasc. Surg.* **2016**, *151*, 841–849, DOI: 10.1016/j.jtcvs.2015.11.043.
- (3) Lobb, R. J.; Becker, M.; Wen, S. W.; Wong, C. S. F.; Wiegmanns, A. P.; Leimgruber, A.; Möller, A. *J. Extracell. Vesicles* **2015**, *4*, DOI: 10.3402/jev.v4.27031.
- (4) Webber, J.; Clayton, A. *J. Extracell. Vesicles* **2013**, *2*, DOI: 10.3402/jev.v2i0.19861.